THE PENNSYLVANIA STATE UNIVERSITY

SCHREYER HONORS COLLEGE

DEPARTMENT OF ELECTRICAL ENGINEERING

DETECTION OF QUADRUPOLE RESONANCE SIGNALS IN THE PRESENCE OF A DETERMINISTIC SINUSOIDAL DISTURBANCE: A COMPARISON OF SIGNAL AVERAGING AND PSEUDO-RANDOM SEQUENCE MODULATION

CATHY YU

Spring 2012

A thesis
submitted in partial fulfillment
of the requirements
for a baccalaureate degree
in Electrical Engineering
with honors in Electrical Engineering

Reviewed and approved* by the following:

Jeffrey L. Schiano
Associate Professor of Electrical Engineering
Thesis Advisor

John D. Mitchell
Professor of Electrical Engineering
Honors Advisor

* Signatures are on file in the Schreyer Honors College.

Abstract

Quadrupole resonance (QR) is a radio frequency (RF) spectroscopy technique that provides a means to non-invasively detect concealed explosives. Applications include inspecting luggage and shoes at aviation security checkpoints. Significant advantages of QR detection systems include the use of non-ionizing radiation and the ability to identify specific explosives, for example, RDX and PETN. The main disadvantage is a small measurement signal-to-noise ratio (SNR) resulting from an inherently small signal amplitude and the presence of RF interference.

This thesis focuses on the detection of QR signals from the explosives PETN and TNT, whose spectral locus is overlapped by AM broadcast stations. Previous research shows that the worst case scenario occurs when the AM broadcast signal derives from a deterministic sinusoidal modulation signal. Unlike the case for uncorrelated thermal noise, signal averaging is not as effective at eliminating the interfering AM signal. This thesis builds upon earlier work where the QR signal is modulated so that it can be distinguished from the RF interference. In specific, for an AM signal using a deterministic modulating signal, this thesis compares the ability of signal averaging and that of QR signal modulation in reducing the effect of AM broadcast interference. Based on analytical analysis and computer simulations, it is shown that modulation of QR signal phase is no more effective than signal averaging in reducing the effect of AM broadcast interference.

Table of Contents

List of Figures

List of Tables

Acknowledgments

I would like to thank Dr. Jeffrey Schiano for his incredible support and endless patience.

Chapter 1

Introduction

1.1 Explosives Detection

Quadrupole resonance (QR) is a radio frequency spectroscopy method that provides a means for revealing the presence of concealed explosives [1]. The application of QR to explosive detection was first proposed during the Vietnam conflict [2]. The need arose for U.S. troops to distinguish improvised explosive devices (IEDs) from decoys. Conventional metal detectors were not effective for IEDs containing only small amounts of metal. An early prototype proved successful in discriminating true IEDs from decoys. However, with the withdrawal of U.S. troops from Vietnam, funding for the QR projects dwindled and interest in the method waned. In December 1988, a minimal-metal explosive device passed through X-ray and metal detectors and lead to the destruction of Pan Am flight 103. The incident led to renewed interest in QR explosive detection technology. Researchers at the Naval Research Laboratory developed a QR test capable of detecting concealed sub-kilogram quantities of explosives [1]. Currently, research is being carried out

Figure 1.1. GE Shoe Scanner

to improve QR detection performance in order to bring the technology into airports and other important security sites for applications such as scanning luggage and shoes [4]. Figure 1.1 shows an QR shoe scanner developed by General Electric.

The physical basis for QR detection systems is the electrostatic interaction between the electric quadrupole moment of nuclei and the electric field gradient resulting from the surrounding electronic charge [5]. This interaction results in preferred orientations of the nucleus. It is possible to change the orientation of the nucleus by applying an external magnetic field whose frequency matches the interaction energy between two preferred orientations. The external magnetic field interacts with the magnetic moment of the nucleus to cause the nucleus to rotate. When the field is removed, the electric quadrupole moment of the nucleus interacts with the surrounding electric field and rotates the nucleus back to a lower energy orientation. As the nucleus possesses a magnetic moment, this motion induces a voltage in the detection coil that reveals the presence of the explosive.

This thesis focuses exclusively on nitrogen-14 (^{14}N) nuclei because most explosives, for instance, PETN, TNT, and RDX, contain nitrogen. Nitrogen-14 nuclei posses intrinsic angular moment, or spin, characterized by a quantum number of

one. As a result, nitrogen-14 nuclei have three preferred orientations. The energy differences among the preferred orientations result in three possible QR transition frequencies. For almost all nitrogen compounds, and hence explosives, the transition frequencies range from 500 KHz to 5 MHz, and are unique among different nitrogen compounds [3]. The latter characteristic allows QR detection systems to both detect and identify explosive material [2] [1]. Of central concern to this thesis is the fact that the transition frequencies for the explosives TNT and PETN lie in the AM broadcast band.

In a QR detection system, a series of radio-frequency (RF) magnetic pulses is generated using the probe coil and applied across the search region. If an explosive compound is present, the energy of a pulse would be absorbed to change the orientation of nitrogen nuclei. Then, in between RF pulses, the electrostatic interaction between nitrogen nuclei and surrounding electronic charges causes nitrogen nuclei to rotate back to an orientation with lower interaction energy. The motion of the nuclear magnetic moment during the inter-pulse interval induces a voltage across the same coil used to excite the response, thereby revealing the presence of the explosive material.

1.2 Detection Strategies

Currently, the effectiveness of QR detection systems is limited. Due to the physical process from which QR responses are generated, the maximum signal amplitude is limited and significantly smaller compared to external noises such as AM broadcast stations. In other words, the signal-to-noise ratio (SNR) of QR measurements is small. In the case of TNT and PETN, the transition frequencies overlap directly with AM broadcast band signals that can be orders of magnitude larger

in amplitude. In this situation,the QR response is masked by the AM broadcast interference.

Previous attempts to reduce the effect of AM broadcast interference include shielding and adaptive noise cancellation [1]. Shielding is a passive strategy. One shielding technique uses a gradiometer coil, such as a figure-eight coil or axial gradiometer. The far-field magnetic interference is reduced by 30 dB and electrical interference pickup is also reduced. As a tradeoff, in comparison to a simple probe, or a magnetometer, the gradiometer produces a smaller output signal in response to a given QR signal [6]. As the name implies, adaptive noise cancellation is an active approach. In addition to the primary probe coil located near the search region, another coil is placed farther away so that it detects the interference but not the QR response. The detected interference is then digitally subtracted from the signal detected by the primary probe. The caveat to this approach is that high dynamic range and careful balancing are needed [7]. Neither shielding or adaptive noise cancellation are adequate in attenuating the AM broadcast interference.

Instead of reducing the level of AM interference, Cosgriff investigated another method which aims to separate the QR signal from the AM interference by modulating the QR signal in a known fashion [8]. Motivated by the use of lock-in detection to improve SNR in CW spectroscopy experiments, Cosgriff approached the QR detection using a similar strategy. The basic idea is to first encode the amplitude and/or the phase of the QR response by modulating a parameter of the RF pulse sequence. Then, the received response is decoded to recover the QR signal.

To demonstrate Cosgriff's approach, suppose a RF pulse sequence is used to generate a series of identical consecutive QR signals separated in time by a repetition period τ. The observed signal is a superposition of both the QR response

and interfering signal. The k^{th} observed signal is represented as

$$r_k(t) = A_q e^{-(t-\tau/2)/T_2^*} \cos(\omega_R t + \theta_k) + n(t + \tau k). \tag{1.1}$$

The first term represents the QR signal as a double-sided exponentially decaying sinusoid with peak amplitude A_q, decay rate T_2^*, frequency ω_R, and phase angle θ_k. The phase angle θ_k can be arbitrarily set by appropriately modifying the parameters of the RF pulse sequence. The value of t for any observation window k ranges from 0 to τ, and the QR signal is centered at $t = \tau/2$. As the interfering noise, n, is in general not the same for each observation window, it is described as a function of $t + \tau k$.

In the case of thermal noise, where $n(t+\tau k)$ arises from electrical losses in the probe coil, signal averaging is used to redue the effect of noise. In this case, the value of θ_k is set to 0 for all k, and the average received signal for N observations is

$$\bar{r}(t) = A_q e^{-|t-\tau/2|/T_2^*} \cos(\omega_R t) + \frac{1}{N} \sum_{k=0}^{N-1} n(t + \tau k). \tag{1.2}$$

The QR signal is not affected by signal averaging because it is identical in every observation window. On the other hand, it can be shown that the root-mean-square of the average noise is $\sqrt{N}$ times smaller than that of the noise in any single observation window [9].

In the case of AM noise, it is well known that signal averaging is not effective in reducing the value of the noise. Applying Cosgriff's method, one approach is to modulate the phase of the excitation sequence and decode the received signal. In specific, Cosgriff suggested randomly choosing θ_k, as either 0 or π, and appropriately multiply $r_k(t)$ by 1 or -1 so that adding the received signals results in

constructive interference of the QR response. Using this approach, the received signal is represented as

$$r_k(t) = b[k]A_q e^{-|t-\tau/2|/T_2^*}\cos(\omega_R t + \theta_k) + b[k]n(t+\tau k) \tag{1.3}$$

where $b[k] = 1$ when $\theta_k = 0$, and $b[k] = -1$ when $\theta_k = \pi$. Choosing $b[k]$ in this fashion, one constructs a composite signal $\bar{r}(t)$ from N observed signals $\bar{r}_k(t)$ as

$$\begin{aligned} \bar{r}(t) &= \frac{1}{N}\sum_{k=0}^{N-1}\bar{r}_k(t) \\ &= A_q e^{-|t-\tau/2|/T_2^*}\cos(\omega_R t) + \frac{1}{N}\sum_{k=0}^{N-1} b[k]n(t+\tau k). \end{aligned} \tag{1.4}$$

Equation 1.4 can be used to represent the composite signal obtained using either averaging where $b[k] = 1$ for all k, or Cosgriff's method where θ_k is a random process that takes on values of either 0 or π. In either approach, the first term representing the QR signal is the same. And so, from the standpoint of investigating the effect of signal averaging and Cosgriff's method on interference reduction, the QR signal can be neglected. In specific, this thesis studies how the energy of the composite noise signal,

$$\bar{n}(t) = \frac{1}{N}\sum_{k=0}^{N-1} b[k]n(t+\tau k), \tag{1.5}$$

is affected using either signal averaging or the QR signal modulation method investigated by Cosgriff.

1.3 Thesis Contributions

The goal of this thesis is to investigate the effect of signal averaging and Cosgriff's approach using phase modulation on a deterministic sinusoidal interference signal. The specific aims of the thesis are to:

1. Obtain closed-form expressions for the average noise signal generated using signal averaging and QR signal modulation.

2. Study the effect of signal averaging and QR signal modulation on the energy of the average noise signal.

3. Verify the analytical predictions using computer simulations.

This thesis extends the work of Cosgriff by providing a detailed comparison of his method against signal averaging for a specific type of interference signal, a deterministic sinusoid.

Chapter 2 analyzes the effect of signal averaging and QR signal modulation on a deterministic sinusoidal interference signal. After defining the interference signal, closed-form expressions for the average noise signal are derived for the case of signal averaging and QR signal modulation. The properties of the random sequence used in QR signal modulation are discussed. Chapter 3 discusses the computer simulations used to verify the prediction results. The closed-from expressions are compared with simulation results. The normalized signal energy plots of the average noise signals obtained using both signal processing methods are also generated. Chapter 4 discusses and summarize the results of this work.

Chapter 2

Analytical Analysis

Section 2.1 describes the deterministic sinusoidal interference signal $n(t)$. Sections 2.2 and 2.3 provide an analytical description of the signal averaging and QR signal modulation techniques. In specific, closed-form expressions are derived for the average noise signals obtained using these methods.

2.1 Representation of AM Interference

Previous work by Cosgriff indicates that in comparison to its thermal noise rejection capability, signal averaging's ability to attenuating sinusoidal interference signals in the received signal is less effective. To simplify the analysis, in particular to avoid complications arising from non-stationary stochastic interference signals, this thesis focuses exclusively on a deterministic sinusoidal disturbance of the form

$$n(t + \tau k) = A_n \cos(2\pi f_o(t + \tau k)), \tag{2.1}$$

where A_n is the peak amplitude of the interference, f_o is the baseband frequency of the disturbance, and τ is the interval time between observed waveforms. In the

analysis of the signal processing algorithms, it will be shown that the phase angle

$$\phi = \pi f_o \tau \tag{2.2}$$

plays an important role. For this reason, the noise signal is expressed as

$$n(t + \tau k) = A_n \cos(2\pi f_o t + 2\phi k). \tag{2.3}$$

For example, if ϕ is an integer multiple of π, then $n(t + \tau k) = n(t)$ for all values of k, that is each observed signal $r_k(t)$ contains the same sinusoidal disturbance.

As discussed in Chapter 1, regardless of the signal processing algorithm used, N measured responses $r_k(t)$ are combined to form a composite signal $\bar{r}(t)$. The component of $\bar{r}(t)$ due just to noise is represented as

$$\bar{n}(t) = \frac{1}{N} \sum_{k=0}^{N-1} b[k] A_n \cos(2\pi f_o t + 2\phi k). \tag{2.4}$$

In the case of signal averaging, the pulse sequence is chosen so that the QR signal phase is the same for all values of k. To recover a composite QR signal from $r_k(t)$, the sequence $b[k]$ is set unity for all values of k. The resulting noise component of the composite signal $\bar{r}(t)$ is defined as

$$\bar{n}_a(t) = \frac{1}{N} \sum_{k=0}^{N-1} A_n \cos(2\pi f_o t + 2\phi k). \tag{2.5}$$

For the case of QR signal modulation, the phase θ_k of the RF pulse is randomly chosen as 0 or π, corresponding to choose $b[k] = +1$ or -1, respectively. From Equation 2.4, the resulting noise component of the composite signal $\bar{r}(t)$ is defined

as

$$\bar{n}_r(t) = \frac{1}{N}\sum_{k=0}^{N-1} b[k]A_n \cos(2\pi f_o t + 2\phi k). \tag{2.6}$$

In section 2.2 and 2.3, it is shown that the signals $\bar{n}_a(t)$ and $\bar{n}_r(t)$ can each be expressed using a single sinusoid

$$\bar{n}_a(t) = A_a \cos(2\pi f_o t + \psi_a) \tag{2.7}$$

$$\bar{n}_r(t) = A_r \cos(2\pi f_o t + \psi_r), \tag{2.8}$$

where the amplitude and phase angle of each expression depend upon the values of the parameters A_n, N, and ϕ.

2.2 Signal Averaging

This section determines the value of the amplitude A_a and phase angle ψ_a for the composite signal $\bar{n}_a(t)$ in Equation 2.7. The key identity used to derive the result is the relationship [10]

$$\sum_{k=0}^{N-1} \cos(x + ky) = \frac{\sin\left(Ny/2\right)}{\sin\left(y/2\right)} \cos\left(x + \frac{N-1}{2}y\right). \tag{2.9}$$

Setting $x = 2\pi f_o t$ and $y = 2\phi$, Equation 2.5 can be expressed as

$$\bar{n}_a(t) = \frac{A_n}{N}\frac{\sin(N\phi)}{\sin(\phi)} \cos(2\pi f_o t + (N-1)\phi). \tag{2.10}$$

Comparing Equation 2.7 and Equation 2.10 reveals that

$$A_a \;=\; \frac{A_n}{N}\frac{\sin(N\phi)}{\sin(\phi)} \tag{2.11}$$

$$\psi_a = (N-1)\phi. \tag{2.12}$$

To simplify the expression for A_a in Equation 2.11, the definition and five relevant properties of the Chebyshev polynomial are introduced [11].

The Chebyshev polynomial of the second kind is defined by the recurrence relationship

$$\begin{aligned} g_0(z) &= 1 \\ g_1(z) &= 2z \\ g_{N+1}(z) &= 2zg_N(z) - g_{N-1}(z) \end{aligned} \tag{2.13}$$

where z is a real number. Alternative notation for $g_N(z)$ includes $U_N(z)$ and $U(N,z)$. For this research,z is set as $\cos(\phi)$ and the six relevant properties are:

P1: $g_{N-1}(\cos\phi) = \sin(N\phi)/\sin(\phi)$ for $N > 1$

P2: $g_{N-1}(\cos\phi)$ is periodic in ϕ with fundamental period π, that is, for any integer ℓ,

$$g_{N-1}(\cos(\phi)) = g_{N-1}(\cos(\phi + \ell\pi)).$$

P3: $g_{N-1}(\cos(\phi))$ is an even (odd) function of $\cos(\phi)$ when $N-1$ is a even (odd) integer, equivalently

$$g_{N-1}(\cos\phi) = (-1)^{N-1} g_{N-1}(-\cos\phi).$$

P4: The largest extrema are achieved at $\cos(\phi) = \pm 1$

$$\begin{aligned} g_{N-1}(1) &= N \\ g_{N-1}(-1) &= N(-1)^{N-1} \end{aligned}$$

P5: $g_{N-1}(\cos\phi)$ has $N+1$ local extrema

P6: $g_{N-1}(\cos\phi)$ has N zeros

These six properties are now used to investigate the values of A_a as a function of the parameters ϕ and N.

Property **P1** allows A_a to be expressed as

$$A_a = \frac{A_n}{N} g_{N-1}(\cos\phi). \tag{2.14}$$

The function $A_a = A_a(N, \phi)$ possess four relevant properties:

PA1: $|A_a| \leq A_n$

PA2: A_a is periodic in ϕ with fundamental period π, that is, for any integer ℓ,

$$A_a(N, \phi) = A_a(N, \phi + \ell\pi)$$

PA3: $|A_a|$ is symmetric about $\phi = \pi/2$ in the sense that

$$|A_a(N, \pi/2 + \phi)| = |A_a(N, \pi/2 - \phi)|$$

PA4: When $\phi = \ell\pi$, where ℓ is an integer,

$$A_a(N, \ell\pi) = A_n$$

Property **PA1** follows directly from property **P4** of the Chebyshev polynomial. Property **PA2** follows directly from property **P2** of the Chebyshev polynomial.

The absolute value of A_a is symmetric about the angle $\phi = \pi/2$. Using Equation 2.14 and property **P3** of the Chebyshev polynomial,

$$\begin{aligned} |A_a(N, \pi/2 + \phi)| &= \frac{A_n}{N} |g_{N-1}(-\cos(\pi/2 + \phi))| \\ &= \frac{A_n}{N} |g_{N-1}(\cos(-\pi/2 + \phi))|. \end{aligned} \tag{2.15}$$

Using the fact that cosine is an even function,

$$\begin{aligned} |A_a(N, \pi/2 + \phi)| &= \frac{A_n}{N} |g_{N-1}(\cos(\pi/2 - \phi))| \\ &= |A_a(N, \pi/2 - \phi)|. \end{aligned} \tag{2.16}$$

Taken together, properties **PA2** and **PA3** show that when determining the energy of the composite signal $\bar{n}_r(t)$, it is only necessary to consider values of ϕ ranging from 0 to $\pi/2$. This is because the energy is directly proportional to the amplitude A_a.

Property **PA4** considers a special case where ϕ is an integer multiple of π, or $\phi = \ell\pi$. From Equation 2.5, it directly follows that

$$\bar{n}_a(t) = A_n \cos(2\pi f_o t). \tag{2.17}$$

As a check, it is now shown that Equation 2.10 gives the same result. First, A_a is determined from Equation 2.14 using L'Hospital's rule

$$A_a = \frac{A_n}{N} \lim_{\phi \to \pi\ell} \frac{\frac{d}{d\phi} \sin(N\phi)}{\frac{d}{d\phi} \sin(\phi)} \tag{2.18}$$

$$= \frac{A_n}{N} \lim_{\phi \to \pi\ell} \frac{N \cos(N\phi)}{\cos(\phi)} \tag{2.19}$$

$$= A_n \frac{\cos(N\pi\ell)}{\cos(\pi\ell)} \tag{2.20}$$

It follows from Equation 2.10 that

$$\bar{n}_a(t) = A_n \frac{\cos(N\ell\pi)}{\cos(\ell\pi)} \cos(2\pi f_o t + (N-1)\ell\pi). \tag{2.21}$$

Equation 2.21 must be evaluated for four cases: (N even, ℓ even), (N odd, ℓ even),

(N odd, ℓ odd), and (N even, ℓ odd). For the first three cases, from Equation 2.20, $A_a = A_n$ and $\psi_a = (N-1)\ell\pi$ is an even multiple of π. Under these conditions, Equation 2.21 simplifies to Equation 2.17. For the last case, from Equation 2.20, $A_a = -A_n$ and $\psi_a = (N-1)\ell\pi$ is an odd multiple of π. Once again, Equation 2.21 simplifies to Equation 2.17. These results show that the expression for $\bar{n}_a(t)$ in Equation 2.10 is consistent with Equation 2.17 for the special case when ϕ is an integer multiple of π.

Properties **P5** and **P6** show that as a function of ϕ, A_a has $N+1$ local extrema and N zeros. As the number of averages N increases, the number of local maxima and zeros increases in a plot of A_a as a function of ϕ.

2.3 QR Signal Modulation

This section determines the value of the amplitude A_r and phase angle ψ_r for the composite signal $\bar{n}_r(t)$ in Equation 2.8. In comparison to the signal averaging approach, where $b[k]$ is unity for all vales of k, QR signal modulation uses a random process $b[k]$ that takes on values of $+1$ and -1 to modulate the phase of the QR response. As a result, the determination of A_r and ψ_r is more challenging. The motivation for employing the random process $b[k]$ is to separate the QR response from the interference, because while $b[k]$ is correlated with the QR response, the AM interference is not.

Following Cosgriff, the random sequence $b[k]$ is realized using a pseudo random sequence (PRS) that is easily generated by recursion. Section 2.3.1 briefly describes the properties of the PRS and the technique for generating the sequence. Section 2.3.2 shows how A_r and ψ_r are derived in terms of the sequence $b[k]$.

2.3.1 Pseudo Random Sequence

The modulation sequence $b[k]$ takes on values $+1$ and -1, and is random in the sense that the value of $b[k]$ is independent of the value of $b[j]$ for all $j \neq k$. It is pseudo random because it is deterministic and after N elements it starts to repeat itself, unlike random sequence. The pseudo random sequence (PRS) is defined by several important properties including [12] [13]

PS1: The PRS $\{b[0], b[1], ..., b[N-1]\}$ has $N = 2^m - 1$ values, where m is an integer

PS2: $b[k]$ is either $+1$ or -1, for $k = 0, 1, ..., N-1$

PS3: The PRS $\{b[0], b[1], ..., b[N-1]\}$ has one more value of $+1$ than -1, and so

$$\sum_{k=0}^{N-1} b[k] = +1$$

PS4: The autocorrelation function of $b[k]$ satisfies

$$R_b[k] = 1/N \sum_{n=0}^{N-1} b[n]b[n+k] = \begin{cases} 1, & k = 0; \\ -1/N, & k \neq 0. \end{cases}$$

The derivation of A_r and ψ_r explicitly uses properties **PS2** and **PS3**. Properties **PS1** and **PS4** help guide the selection of sequence lengths used in computer simulations presented in Chapter 3.

The selection of the sequence length N determines the QR detection time and the value of the autocorrelation function $R_b[k]$ for $k \neq 0$. The QR detection time is the product of the number, N, of QR signals acquired and the duration, τ, of the acquisition of each signal. In general, it is desirable to use a small value of N to minimize the detection time $N\tau$. On the other hand, for values of k other than zero, the autocorrelation function has the value of $-1/N$. A conjecture

of Cosgriff's research is that detection performance improves as the magnitude of the autocorrelation function, $R_b[k]$, decreases for values of $k \neq 0$. From this consideration, a large value of N is useful. And so there exists a tradeoff between detection time and detection performance. For this thesis, values of 511, 127, and 15 are used for N, corresponding to detection time of 1.022s, 434ms, and 30ms using a pulse spacing of τ of 2ms.

This thesis generates a PRS $b[k]$ of length N from a pseudo binary random sequence $a[k]$ of length N as

$$b[k] = 2a[k] - 1, \tag{2.22}$$

where $a[k]$ takes on the binary values of 0 and 1 [12] [13]. The binary sequence $a[k]$ is generated recursively using a cascade combination of m delay elements to produce a sequence of length $N = 2^m - 1$. The output of the m^{th} delay element represents $a[k]$. The input to the 1^{st} delay element is the modulo 2 sum of the output of two of the delay elements. The modulo 2 summer is equivalent to the exclusive-or operation for binary numbers. The location of the feedback taps depends on the sequence length. The initial state of each delay element is arbitrary, but at least one delay element must have an initial state of 1. For this thesis, the initial state of all m delay element is set to 1. Figure 2.1(A) through 2.1(C) show the feedback system for generating $a[k]$ using sequence lengths of 15, 127, and 511, respectively.

2.3.2 Pseudo Random Sequence Modulation

The values of the amplitude A_r and phase angle ψ_r for the composite signal $\bar{n}_r(t)$ in Equation 2.8 are now determined. From Equation 2.6, $\bar{n}_r(t)$ is a summation of

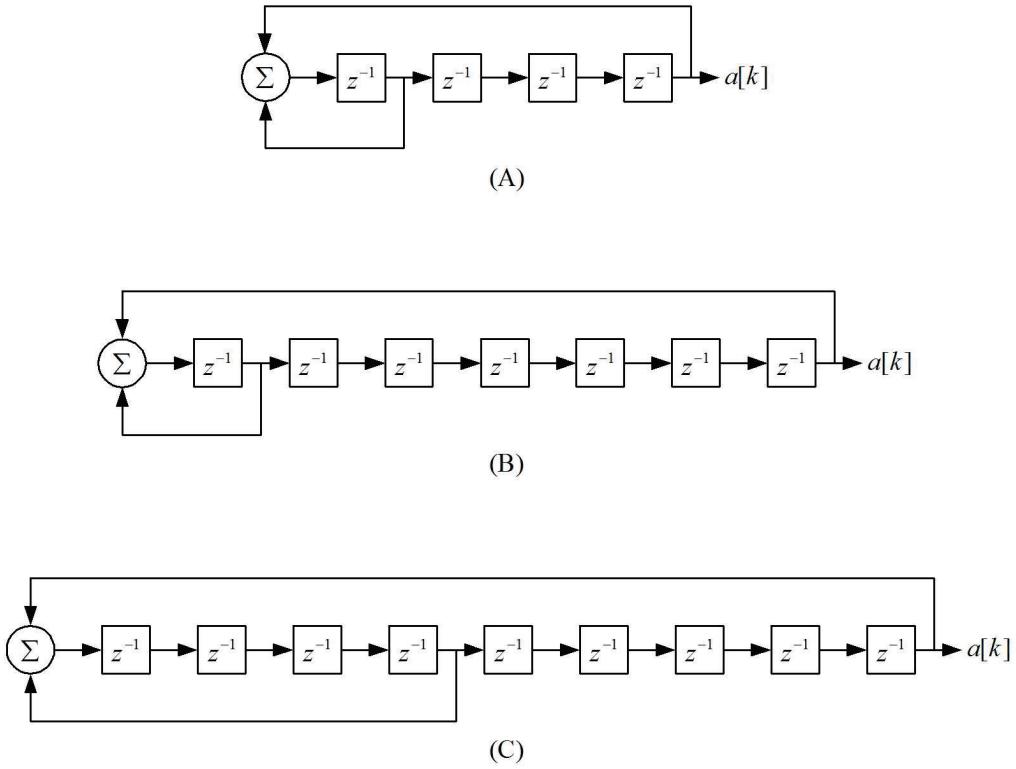

Figure 2.1. Discrete-Time Systems for PRS Generation

sinusoids of the same frequency and so it can be represented using phasor analysis. The phasor representation of $\bar{n}_r(t)$ with respect to the frequency $2\pi f_o$ is the complex-valued constant

$$\hat{N}_r = \frac{1}{N}\sum_{k=0}^{N-1} A_n e^{-j2\phi k} b[k]. \tag{2.23}$$

The magnitude of the phaser $\hat{N}_r$ represents A_r and is

$$A_r = |\hat{N}_r| = \frac{A_n}{N}\left|\sum_{k=0}^{N-1} e^{-j2\phi k} b[k]\right|, \tag{2.24}$$

where A_n and N are positive constants. The angle of the phasor $\hat{N}_r$ represents ψ_r and is given by

$$\psi_r = \angle \hat{N}_r = \angle \sum_{k=0}^{N-1} e^{-j2\phi k} b[k]. \tag{2.25}$$

In determining the energy of the composite signal $\bar{n}_r(t)$, only the amplitude A_r is of concern.

The amplitude $A_r = A_r(N, \phi)$ is now shown to possess four properties:

PR1: $A_r \leq A_n$

PR2: A_r is periodic in ϕ with fundamental period π, that is for any integer ℓ

$$A_r(N, \phi) = A_r(N, \phi + \ell\pi). \tag{2.26}$$

PR3: A_r is symmetric about $\phi = \pi/2$ in the sense that

$$A_r(N, \pi/2 + \phi) = A_r(N, \pi/2 - \phi). \tag{2.27}$$

PR4: When $\phi = \ell\pi$, where ℓ is an integer,

$$A_r(N, \ell\pi) = A_n/N. \tag{2.28}$$

Property **PR1** is obtained by applying the triangle equality to Equation 2.24

$$A_r = \frac{A_n}{N} \left| \sum_{k=0}^{N-1} e^{-j2\phi k} b[k] \right| \leq \frac{A_n}{N} \sum_{k=0}^{N-1} \left| e^{-j2\phi k} b[k] \right|. \tag{2.29}$$

Using the fact that

$$\sum_{k=0}^{N-1} \left| e^{-j2\phi k} b[k] \right| = \sum_{k=0}^{N-1} 1 = N, \tag{2.30}$$

immediately yields

$$A_r \leq A_n. \tag{2.31}$$

This result shows that the amplitude of the composite noise signal $\hat{n}_r(t)$ is always less or equal to the noise amplitude for any single observed $r_k(t)$.

It is now shown that $A_r(N,\phi)$ is a periodic function in ϕ with fundamental period π as described in property **PR2**. From Equation 2.24

$$A_r(N,\phi+\ell\pi) = \frac{A_n}{N}\left|\sum_{k=0}^{N-1} e^{-j2(\phi+\ell\pi)k} b[k]\right| \tag{2.32}$$

$$= \frac{A_n}{N}\left|\sum_{k=0}^{N-1} A_n e^{-j2\phi k} b[k] e^{-j2\ell k\pi}\right| \tag{2.33}$$

As $e^{-j2\ell k\pi} = 1$ for all integers ℓ and k, it immediately follows that

$$A_r(N,\phi+\ell\pi) = A_r(N,\phi). \tag{2.34}$$

Observe that the same property holds for A_a.

The third property **PR3** is shown by expressing A_r from Equation 2.24 as

$$A_r(N,\pi/2+\phi) = \frac{A_n}{N}\left|\sum_{k=0}^{N-1} e^{-j2(\pi/2+\phi)k} b[k]\right| \tag{2.35}$$

$$= \frac{A_n}{N}\left|\sum_{k=0}^{N-1} e^{-j2k\pi} e^{-j2(-\pi/2+\phi)k} b[k]\right|. \tag{2.36}$$

Using the facts that $e^{-j2k\pi} = 1$ for all integers k and that taking the complex conjugate of the summation will not change its magnitude yield

$$A_r(N,\pi/2-\phi) = \frac{A_n}{N}\left|\sum_{k=0}^{N-1} e^{-j2(\phi-\pi/2)k} b[k]\right| \tag{2.37}$$

$$= A_r(N,\phi-\pi/2). \tag{2.38}$$

The last equality shows that the amplitude A_r is symmetric about $\phi = \pi/2$.

To prove property **PR4** set $\phi = \ell\pi$ where ℓ is an integer. Using Equation 2.24,

$$A_r(N, \ell\pi) = \frac{A_n}{N} \left| \sum_{k=0}^{N-1} e^{-j2(\ell\pi)k} b[k] \right|. \tag{2.39}$$

As $e^{-j2\ell k\pi} = 1$ for all integers ℓ and k,

$$A_r(N, \ell\pi) = \frac{A_n}{N} \left| \sum_{k=0}^{N-1} b[k] \right|. \tag{2.40}$$

Using property **PS3** of the PRS,

$$A_r(N, \ell\pi) = \frac{A_n}{N}. \tag{2.41}$$

When ϕ is an integer multiple of π, the amplitude of the noise $\bar{n}_r(t)$ is N times smaller than the noise amplitude for any received signal $r_k(t)$.

Chapter 3

Computer Simulations

3.1 Verification of Noise Models

Computer simulations are used to verify the closed-form expressions for the composite noise signals generated using signal averaging and QR signal modulation. In specific, the composite signals $\bar{n}_a(t)$ and $\bar{n}_r(t)$ given by Equation 2.5 and 2.6, respectively, are determined by computer simulations. These signals are then compared against the signals $\bar{n}_a(t)$ and $\bar{n}_r(t)$ produced by Equation 2.7 and 2.8, respectively. If the analytical calculations in Chapter 2 are correct, the predicted and simulated signals must match exactly.

In the computer simulations, the values of N and τ are chose as 511 and 2ms, respectively, to match typical values in a QR detection experiment. The baseband frequency f_o is chose as 0.0278kHz to produce an angle ϕ of 10°. The resulting value of A_a is determined using the MATLAB function $mfun$ that realizes the Chebyshev polynomial. For QR signal modulation, the PRS $b[k]$ is generated recursively using the system in Figure 2.1(C) with the initial condition of all $m = 9$ delay elements set to unity. For convenience, the amplitude A_n is set to unity.

Figure 3.1 shows the simulated and predicted signals $\bar{n}_a(t)$ obtained using signal averaging over the interval $0 < t < 1ms$. The solid curve shows the predicted value of $\bar{n}_a(t)$, while the solid curve masked with open circles indicates the simulated value of $\bar{n}_a(t)$. As expected, the curves match exactly.

Figure 3.2 shows the simulated and predicted signal $\bar{n}_r(t)$ obtained using QR signal modulation over the interval $0 < t < 1ms$. The solid curve shows the predicted value of $\bar{n}_r(t)$, while the solid curve masked with open circles indicates the simulated value of $\bar{n}_r(t)$. As expected, the curves match exactly.

Because Figure 3.1 and Figure 3.2 are generated in an identical fashion except for the method used to compute the composite noise signal, it is of value to compare the relative amplitude of the sinusoids in the two figures. Observe that the amplitude of the composite signal obtained using signal averaging is more than ten times smaller than the composite signal using QR signal modulation. For the case of $N = 511$ and $\phi = 10°$, Figure 3.1 and Figure 3.2 show that the signal averaging method is superior to that of QR signal modulation for reducing the amplitude of the sinusoidal interference signal. Section 3.2 compares the performance of the signal averaging method against QR signal modulation as a function of the parameters N and ϕ.

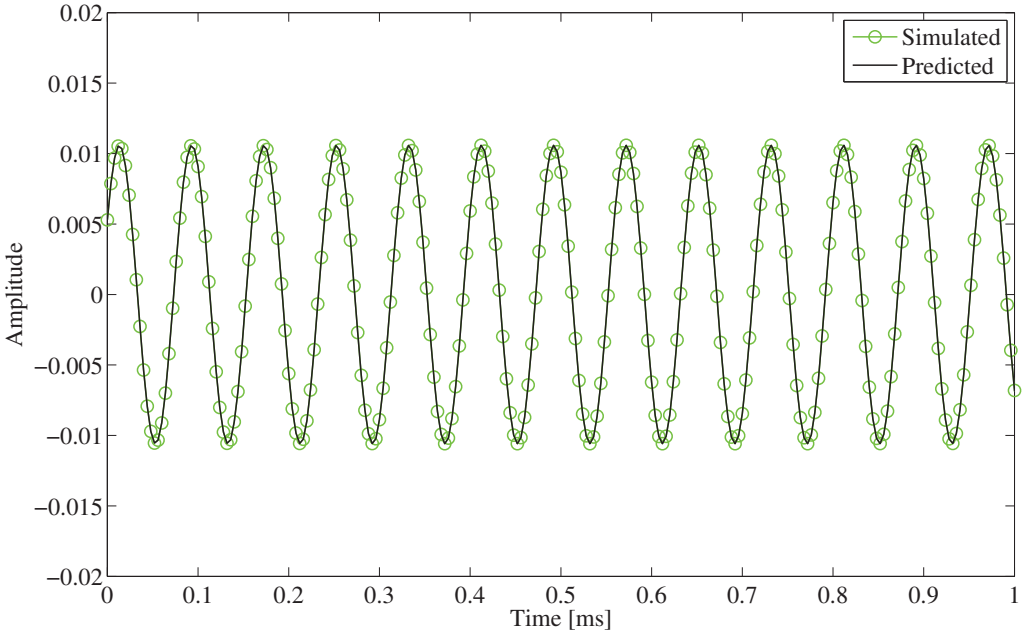

Figure 3.1. Plot of $\bar{n}_a(t)$ for A_n=1, ϕ= 10°, N=511

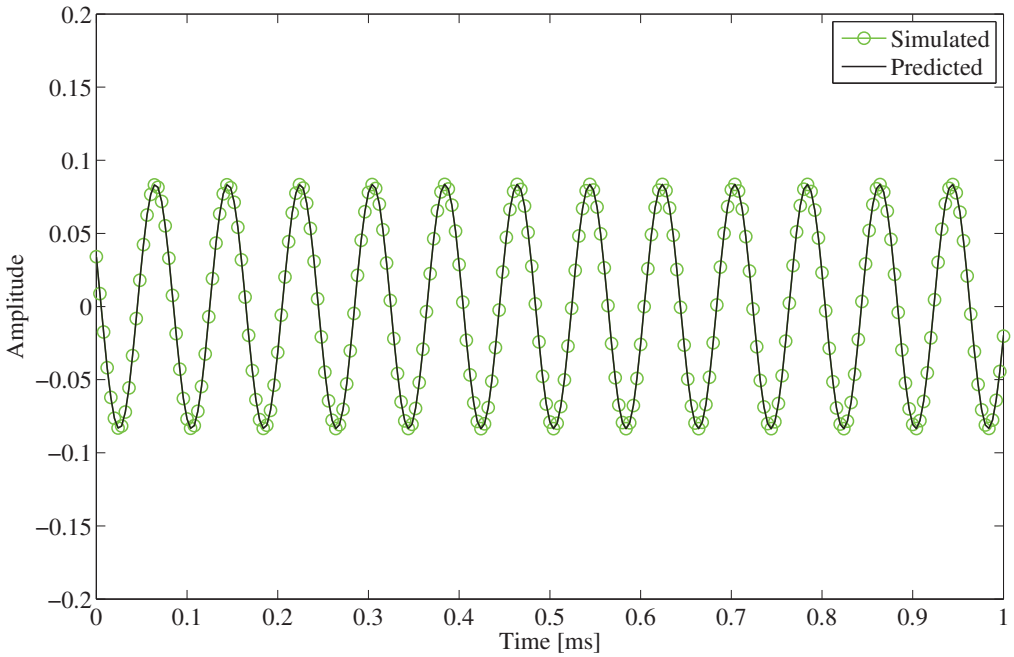

Figure 3.2. Plot of $\bar{n}_r(t)$ for A_n=1, ϕ= 10°, N=511

3.2 Investigation of Noise Energy

In QR Detection systems, the energy of the composite signal is typically compared against a threshold value to determine the presence or absence of an explosive device. To reduce the number of false alarms, it is desirable that the energy of the composite noise signal be as small as possible. This section compares the energy of the composite noise signals using signal averaging and QR signal modulation as a function of the number averages N and the angle $\phi = \pi f_o \tau$.

The energy E_a and E_r of the composite noise signals $\bar{n}_a(t)$ and $\bar{n}_r(t)$ are taken as A_a^2 and A_r^2, respectively. It follows from Equation 2.11 and 2.24 that

$$E_a = \left(\frac{A_n}{N} \frac{\sin(N\phi)}{\sin(\phi)} \right)^2 \tag{3.1}$$

$$E_r = \left(\frac{A_n}{N} \left| \sum_{k=0}^{N-1} e^{-j2\phi k} b[k] \right| \right)^2. \tag{3.2}$$

For convenience, the value of A_n is set to unity. The performances of signal averaging and QR modulation method are compared by investigating the energies E_a and E_r as a function of N and ϕ.

For this study, the number of averages N ranges from 1 to 511. The upper value of N represents a detection time of approximately 1s for a pulse spacing τ of 2ms. Because of properties **PA3** and **PR3**, it is only necessary to consider the values of E_a and E_r over the interval $0 < \phi < \pi/2$. When ϕ is zero, and with A_n set to unity, properties **PA4** and **PR4** show that $E_a = 1$ and $E_r = 1/N^2$. In addition to determining the values of E_a and E_r for $\phi = 0$ and 90^o, values of 1^o and 10^o are also used to study the behavior of the noise energy when ϕ is close to zero.

Figure 3.3 shows a plot of the energy E_a as a function of N. The star, open

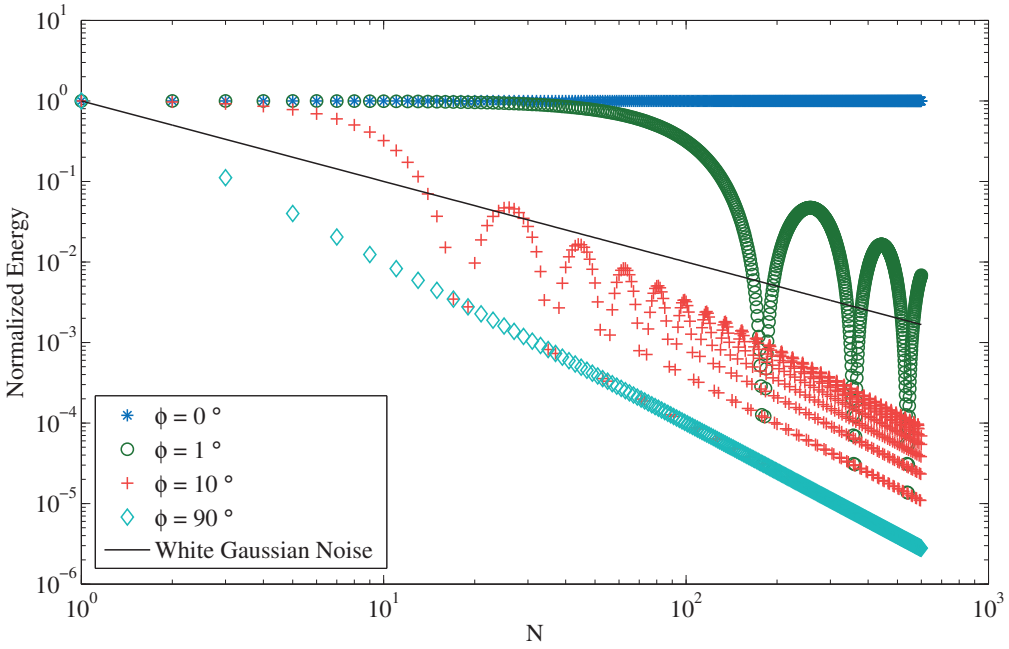

Figure 3.3. Normalize Signal Energy Using Signal Averaging

circle, plus, and open diamond show the value of E_a when ϕ is set to 0^o, 1^o, 10^o, and 90^o, respectively. As a benchmark, also shown is a solid curve representing the energy of the composite signal when the noise is a white Gaussian process. The variance of the Gaussian process is chosen so that the noise energy is unity when N is one. The energy of the composite signal derived from the Gaussian white process decreases as $1/N$.

When ϕ is zero, the energy E_a is independent of N. In this case, signal averaging affords no improvement in reducing the energy of the noise signal. When ϕ is increased to 1^o, the energy E_a begins to decrease only when the number of averages grows large. When ϕ is increase to 10^o, for values of N beyond 10, signal averaging decreases the energy of the sinusoid disturbance at a rate greater than $1/N$. This effect is more pronounced when ϕ is 90^o.

Figure 3.4 shows a plot of the energy E_r as a function of N. Once again, the

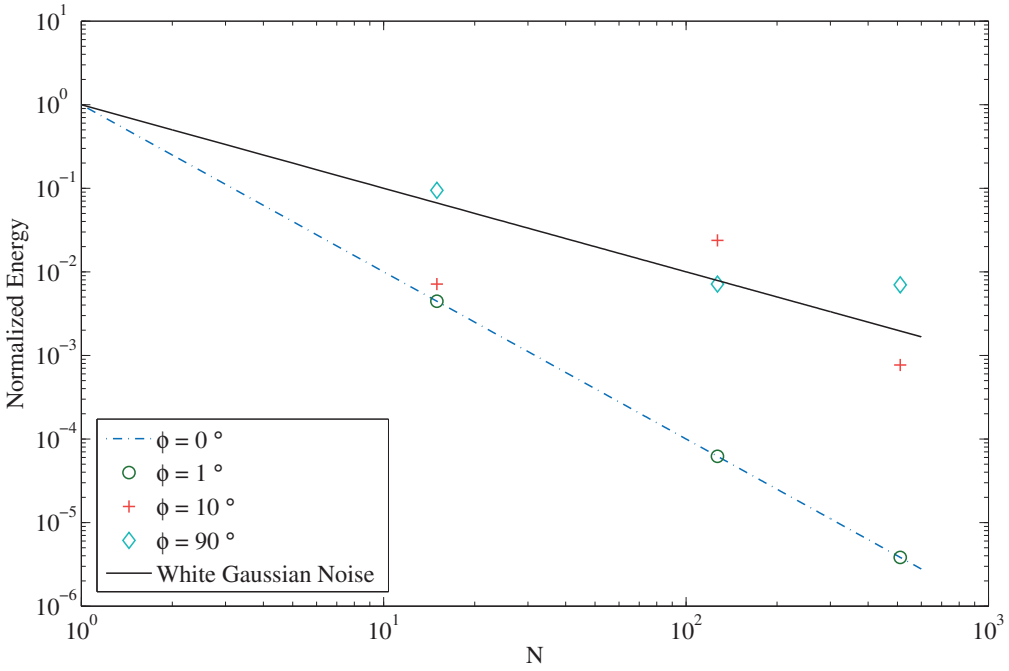

Figure 3.4. Normalized Signal Averaging Using QR Signal Modulation

solid curve shows the behavior of signal energy for the case of signal averaging on a white Gaussian noise source. The dashed-line shows E_r of a function of N when ϕ is set to 0^o. The circle, plus, and diamond show E_r when ϕ is set to 0^o, 1^o, 10^o, and 90^o, respectively. For these three values of ϕ, E_r is computed for N set to 15, 127, and 511.

When ϕ is 0^o, Figure 3.4 shows that QR signal modulation reduces the energy of the sinusoid disturbance at a rate greater than $1/N$. However, as ϕ increases toward 90^o, QR signal modulation becomes less effective at reducing the energy of the composite noise signal $\bar{n}_r(t)$.

A comparison of Figure 3.3 and 3.4 suggests that QR signal modulation is superior to signal averaging when $\phi = 0$. However, by using the method of phase cycling, the signal averaging method can completely eliminate the sinusoid disturbance when $\phi = 0$ [8].

Chapter 4

Discussion and Summary

This thesis investigates the effect of using signal averaging and QR signal modulation on deterministic sinusoidal disturbances. The analytic analysis in Chapter 2 reveals that signal averaging and QR signal modulation behave similarly. Table 4 shows the relevant properties of the noise amplitude A_a and A_r observed using signal averaging and QR signal modulation, respectively. Properties **PA1** and **PR1** show that the upper bound on the composite noise amplitude is A_n for both signal averaging and QR signal modulation. Properties (**PA2**,**PA3**) and (**PR2**,**PR3**) shows that it is only necessary to consider the signal energy E_a and E_r as a function of ϕ over the interval $0 < \phi < \pi/2$.

The most significant difference between signal averaging and QR signal modulation is revealed by properties **PA4** and **PR4**. Property **PA4** shows that signal

Signal Averaging	**QR Signal Modulation**
PA1 :$\lvert A_a \rvert \leq A_n$	**PR1** :$A_r \leq A_n$
PA2 :$A_a(N,\phi) = A_a(N,\phi+\ell\pi)$	**PR2** :$A_r(N,\phi) = A_r(N,\phi+\ell\pi)$
PA3 :$\lvert A_a(N,\pi/2+\phi)\rvert = \lvert A_a(N,\pi/2-\phi)\rvert$	**PR3** :$A_r(N,\pi/2+\phi) = A_r(N,\pi/2-\phi)$
PA4 :$A_a(N,\ell\pi) = A_n$	**PR4** :$A_r(N,\ell\pi) = A_n/N$

Table 4.1. Properties of A_a and A_r

averaging has no effect on the noise amplitude A_a, and thus no effect on the noise energy E_a when ϕ is an integer multiple of π. In contrast, for QR signal modulation, when ϕ is an integer multiple of π, the signal energy E_r decreases with $1/N$. However, for the case of $\phi = 0$, phase-cycling can be used in conjunction with signal averaging to reduce the energy of the composite noise signal to zero [8].

Table 4.2 compares the signal energy E_a and E_r for ϕ set to 0^o, 1^o, 10^o, and 90^o, and for values of N equal to 15, 127, and 511. When ϕ is 0^o or 1^o, it is shown that the QR signal modulation provides a greater reduction in the composite noise energy than does signal averaging. However, for larger values of ϕ, signal averaging provides a great reduction in the noise energy.

Based on the results of the thesis, there is no clear advantage for using QR signal modulation over signal averaging to reduce the energy of the composite noise signal associated with a sinusoidal disturbance. On the other hand, this thesis only considers the modulation the phase of the QR signal. Further research is needed to determine if QR amplitude modulation can be used to decrease the effect of sinusoidal interference signals on QR signal detection.

	$N = 15$		$N = 127$		$N = 511$	
ϕ [deg]	E_a	E_r	E_a	E_r	E_a	E_r
0	1	0.0044	1	$6.3E-5$	1	$3.8E-6$
1	0.98	0.0044	0.13	$6.2E-5$	0.0039	$3.8E-6$
10	0.037	0.0071	$6.2E-5$	0.024	0.00011	0.00077
90	0.0044	0.094	$6.2E-5$	0.0071	$3.8E-6$	0.0007

Table 4.2. Dependence of Composite Signal Energy on ϕ and N

Bibliography

[1] A. N. Garroway, M. L. Buess, J. B. Miller, B. H. Suits, A. D. Hibbs, G. A. Barrall, R. Matthews, and L. J. Burnett. "Remote Sensing by Nuclear Quadrupole Resonance." IEEE Transactions on Geoscience and Remote Sensing, vol. 39, pp. 1108-1118, 2001.

[2] T. Hirschfeld. "Short Range Remote NQR Measurements." Journal of Molecular Structure, vol. 58, pp. 63-77, 1980.

[3] J. P. Yesinowski, M. L. Buess, and A. N. Garroway. "Detection of ^{14}N and ^{35}Cl in Cocaine Base and Hydrochloride Using NQR, NMR, and SQUID Techniques." Analytical Chemistry, vol. 67 pp. 2256-2263, 1995.

[4] C. Crowley, T. Petrov, O. Mitchell, R. Shelby, L. Ficke, S. Kumar and P. Prado. "A Novel Shoe Scanner Using an Open-Access Quadrupole Resonance and Metal Sensor." Sensors, and Command, Control, Communications, and Intelligence (C3I) Technologies for Homeland Security and Homeland Defense, vol. 6538, 2007.

[5] J. A. Smith. "Nuclear Quadrupole Resonance Spectroscopy." Journal of Chemical Education, vol. 48, pp. 39-49, 1971.

[6] B. H. Suits. "The Noise Immunity of Gradiometer Coils for ^{14}NNOR Land Mine Detection: Practical Limitations." Applied Magnetic Resomance, vol. 25, pp. 371-382, 2004.

[7] S. Tantum, L. Collins, L. Carin. "Signal Processing for NOR Discrimination of Buried Landmines." SPIE Conference on Detection and Remediation Technologies for Mines and Minelike Targets, vol. 3710, pp. 474-482, 1999.

[8] R. J. Cosgriff, "Detection of Quadrupole Resonance in Noise by Encoding the Pulse Sequence Parameters and Decoding the Measure Responses." Honors thesis, Department of Electrical Engineering, The Pennsylvania State University, University Park, PA, 2009.

[9] R. R. Ernst. "Sensitivity enhancement in magnetic resonance." Review of Scientific Instruments, vol. 36, pp. 1689-1695, 1965.

[10] I.S. Gradshteyn, I.M.Ryzhik. *Table of Integrals, Series, and Products*, Academic Press. pp. 29, 1994.

[11] J.C. Mason, D.C.Handscomb. *Chebyshev Polynomials*, Chapman and Hall/CRC. 2003.

[12] W.D.T. Davies. *System Identification for Self-Adaptive Control*, Wiley-Interscience., 1970.

[13] F.J. MacWilliams, N.J. Sloane "Pseudo-Random Sequences and Arrays." Proceedings of the IEEE, vol. 64, pp. 1715-1729, 1976.

Chapter 5

Academic Vita

Name: Cathy Yu

Address: 623 West Calder Way Unit 2
State College, PA 16801

Email: xvy5016@psu.edu

Education:
The Pennsylvania State University, University Park, PA
B. S. in Electrical Engineering, May 2012

Honors: Schreyer Honors College Scholar
Dean's list every semester

Thesis Title: *Detection of Quadrupole Resonance Signals in the Presence of a Deterministic Sinusoidal Disturbance: A Comparison of Signal Averaging and Pseudo-Random Sequence Modulation*

Thesis Supervisor: Jeffrey L. Schiano
Associate Professor of Electrical Engineering

Work Experience:

June 2011 - August 2011
Gas & Power Marketing Intern
ExxonMobil Corporation, Houston, TX
Supervisor: Brian Sellers
- Spearheaded strategy optimization project for natural gas transportation to maximize value captured on current contracts and guide future contract negotiations
- Identified and recovered $85,000/year plus $50,000 one-time refund from 3rd party
- Created and captured pipeline knowledge and associated cost structure insights in desk manuals, supply models, and training decks
- Gained base knowledge of treasury rates products, systems, and infrastructure

June 2010 - August 2010
Investment Banking eTrading Intern
JP Morgan Chase & Co., New York, NY
Supervisor: Daniel Hennessy
- Interfaced as the liaison between New York office and the new India IT team to develop daily eTrading automated testing, saving an annual 60 days of manual testing time
- Developed a single message parser as the core component of intelligent data comparison for automated testing use across all products
- Gained base knowledge of treasury rates products, systems, and infrastructure

June 2009 - August 2009
Renewal Parts Proposal Intern
General Electric Company, Erie, PA
Supervisor: Jeffrey P Mennini
- Nominated target buyers and preliminary pricing for $20 million excess inventory
- Improved material availability by 18% for the $15 million India 45 Kits program

Awards:
- Xerox Technical Minority Scholarship (2011)
- Greater Cleveland Chapter of the PSU Alumni Association Scholarship (2010)
- AMETEK Outstanding Student Award (2010)